Comparative Study of CO₂ Capture by Carbon Nanotubes, Activated Carbons, and Zeolites

Chungsying Lu,*,† Hsunling Bai,‡ Bilen Wu,† Fengsheng Su,† and Jyh Feng Hwang§

Department of Environmental Engineering, National Chung Hsing University, Taichung 402, Taiwan, Institute of Environmental Engineering, National Chiao Tung University, Hsinchu 300, Taiwan, and Fuel Utilization Laboratory, Industrial Energy Conservation Technology Division, Energy and Environment research Laboratories, Industrial Technology Research Institute, Hsinchu 310, Taiwan

Carbon nanotubes (CNTs), granular activated carbon (GAC), and zeolites were modified by 3-aminopropyl-triethoxysilane (APTS) and were selected as adsorbents to study their physicochemical properties and adsorption behaviors of CO₂ from gas streams. The surface nature of these adsorbents was changed after the modification, which make them adsorb more CO₂ gases. Under the same conditions, the modified CNTs possess the greatest adsorption capacity of CO₂, followed by the modified zeolites and then the modified GAC. The mechanism of CO₂ adsorption on these adsorbents appears mainly attributable to physical force, which makes regeneration of spent adsorbents at a relatively low temperature become feasible. The APTS-modified CNTs show good performance of CO₂ adsorption as compared to many types of modified carbon and silica adsorbents reported in the literature. This suggests that the APTS-modified CNTs are efficient CO₂ adsorbents and that they possess potential applications for CO₂ capture from gas streams.

Introduction

The CO₂ capture and storage (CCS) technologies from combustion gases are concerning after the Kyoto Protocol came into force on February 16, 2005. Various CO₂ capture technologies, including absorption, adsorption, cryogenics, membranes, and so forth, have been investigated.[1,2] Among them, the absorption−regeneration technology has been recognized as the most matured process so far, with the amine-based or ammonia-based absorption processes receiving the greatest attention.[3–5]

However, because the energy penalty of the absorption process is still too high, other technologies are being investigated throughout the world. The Intergovernmental Panel on Climate Change (IPCC) special report concluded that the design of a full-scale adsorption process might be feasible and the development of a new generation of materials that would efficiently adsorb CO₂ will undoubtedly enhance the competitiveness of adsorptive separation in a flue gas application.[6] Possible adsorbents include activated carbon,[7,8] zeolites,[9,10] silica adsorbents,[11,12] single-walled carbon nanotubes (SWCNTs),[13]

and a nanoporous silica-based molecular basket.[14,15] However, a systematic comparison on the CO₂ capture with these adsorbents is still very limited in the literature.

This article investigates the physicochemical properties of raw and 3-aminopropyl-triethoxysilane (H₂NCH₂CH₂CH₂−Si(OCH₂CH₃)₃, abbreviated as APTS) modified carbon nanotubes (CNTs), granular activated carbon (GAC), and zeolites. A comparative study on the adsorption behavior of CO₂ from gas streams with these adsorbents is also given.

Experimental Section

1. Adsorbents. Commercially available multiwalled CNTs with inner diameter < 10 nm (L-type, Nanotech Port Co., Shenzhen, China), zeolites with unit cell size of 24.7 Å (CBV100, Zeolyst International, Valley Forge, U.S.A.), and GAC with particle diameter range of 0.55−0.75 mm (Filtrasorb 400, Calgon Carbon Co., Tianjia, China) were selected as adsorbents in this study. The length of CNTs was in the range of 5−15 μm, and the amorphous carbon content in CNTs was <5 wt %. The SiO₂/Al₂O₃ mole ratio of zeolites was 5.1. These data were provided by the manufacturer.

Raw adsorbents were thermally pretreated in a furnace at 300 °C by passing N₂ gas for 60 min. After the thermal treatment, these

* To whom correspondence should be addressed. E-mail: clu@nchu.edu.tw. Fax: +886-4-22862587.
† National Chung Hsing University.
‡ National Chiao Tung University.
§ Industrial Technology Research Institute.

(1) White, C. M.; Strazisar, B. R.; Granite, E. J.; Hoffman, J. S.; Pennline, H. W. *J. Air Waste Manage. Assoc.* **2003**, *53* (6), 645–715.
(2) Aaron, D.; Tsouris, C. *Sep. Sci. Technol.* **2005**, *40* (1−3), 321–348.
(3) Bai, H. L.; Yeh, A. C. *Ind. Eng. Chem. Res.* **1997**, *36* (6), 2490–2493.
(4) Yeh, A. C.; Bai, H. L. *Sci. Total Environ.* **1999**, *228* (2−3), 121–133.
(5) Rao, A. B.; Rubin, E. S. *Environ. Sci. Technol.* **2002**, *36* (20), 4467–4475.
(6) Intergovernmental Panel on Climate Change (IPCC). Special Report on Carbon dioxide Capture and Storage. http://www.ipcc.ch/activity/srccs/index.htm (2005).
(7) Siriwardane, R. V.; Shen, M. S.; Fisher, E. P.; Losch, J. *Energy Fuels* **2001**, *15* (2), 279–284.

(8) Prezepiórski, J.; Skrodzewicz, M.; Morawski, A. W. *Appl. Surf. Sci.* **2004**, *225* (1−4), 235–242.
(9) Gao, W.; Butler, D.; Tomasko, D. L. *Langmuir* **2004**, *20* (19), 8083–8089.
(10) Siriwardane, R. V.; Shen, M. S.; Fisher, E. P.; Poston, J. A. *Energy Fuels* **2005**, *19* (3), 1153–1159.
(11) Gray, M. L.; Soong, Y.; Champagne, K. J.; Pennline, H.; Baltrus, J. P., Jr.; Khatri, R.; Chuang, S. S. C.; Filburn, T. *Fuel Process. Technol.* **2005**, *86* (14−15), 1449–1455.
(12) Hiyoshi, N.; Yogo, K.; Yashima, T. *Microporous Mesoporous Mater.* **2005**, *84* (1−3), 357–365.
(13) Cinke, M.; Li, J., Jr.; Ricca, A.; Meyyappan, M. *Chem. Phys. Lett.* **2003**, *376* (5−6), 761–766.
(14) Xu, X. C.; Song, C.; Andresen, J. M.; Miller, B. G.; Scaroni, A. W. *Energy Fuels* **2002**, *16* (6), 1463–1469.
(15) Xu, X. C.; Song, C. S.; Miller, B. G.; Scaroni, A. W. *Ind. Eng. Chem. Res.* **2005**, *44* (21), 8113–8119.
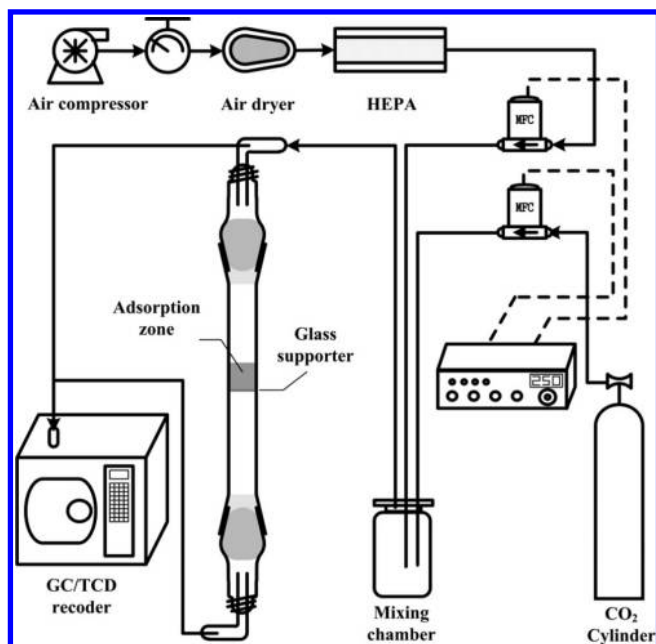
Figure 1. Diagram of the experimental setup.

adsorbents were dispersed into flasks containing various kinds of chemical agents (Riedel deHäen, Analytical Reagent, Seelze, Germany) including 30% monoethanolamine (MEA), 30% NH_3(aq), and 10% APTS (90 mL of 99.8% purity toluene + 10 mL of 97% purity APTS) to determine the optimum modification method of employed adsorbents for enhancing CO_2 capture. Literature screening indicates that these chemical agents show potential to modify carbon adsorbents[8] or silica adsorbents.[11,12] The mixture was then refluxed at the boil for 24 h. After cooling to room temperature, the mixture was filtered through a 0.45 μm fiber filter, and the solid was dehydrated in an oven at 105 °C for 2 h and then was dried in a furnace at 110 °C for 2 h by the passage of N_2 gas.

2. Adsorption Experiment. The experimental setup for CO_2 adsorption is shown in Figure 1. The adsorption column was made of Pyrex glass, with a total length of 20 cm and an internal diameter of 1.5 cm. The column was filled with 1.0 g of adsorbents (packing height ≈ 3.5 cm) and placed within a temperature control box (Model CH-502, Chin Hsin, Taipei, Taiwan) to maintain a constant temperature at 25 °C.

Compressed air was passed first through a silica gel air dryer to remove moisture and oil and then was passed through a HEPA filter (Gelman Science, Ann Arbor, MI, U.S.A.) to remove particulates. The clean air was then served as a diluting gas and was mixed with pure CO_2 gas obtained from a pure CO_2 cylinder (99.9% purity) before entering the absorption column. The influent CO_2 concentration and the system flow rate were controlled via mass flow controllers (model 247C four channel read-out and model 1179A for mass flow controller, MKS Instrument Inc., MA, U.S.A.). The mixed gas was then passed downward into the adsorption column. The influent and effluent gas streams were flowed into a gas chromatograph (GC) equipped with a thermal-conductivity detector (TCD) by an autosampling system. The influent CO_2 concentration was in the range of 5–50%, which was selected to be representative of different CO_2 levels in combustion gases from many kinds of industrial activities, fossil fuel power plants, or coal gasification system. The variations in the influent CO_2 concentration were below 0.2%, and the system flow rate was controlled at 0.08 L/min which is equivalent to an empty-bed retention time of 4.6 s.

The amount of CO_2 adsorbed on adsorbents (q, mg/g) at a certain time (t, min) was calculated as

$$q = \frac{1}{m}\int_0^t Q(C_{in} - C_{eff})\,dt \qquad (1)$$

where m is the weight of virgin adsorbents (g); Q is the influent flow rate (L/min); and C_{in} and C_{eff} are the influent and effluent

CO_2 concentrations (mg/L), respectively.

3. Physisorption and Chemisorption. Most adsorption processes are a combination of physical force (physisorption) and chemical force (chemisorption). Physisorption occurs due to van der Waals forces between adsorbate molecules and adsorbents while chemisorption takes place due to chemical interactions between the adsorbate molecules and the surface functional groups of adsorbents. A distinction of these two processes is very useful in understanding the factors that influence the rate of adsorption process. The equilibrium amount of CO_2 adsorbed on adsorbents due to physisorption (q_{ep}, mg/g) and chemisorption (q_{ec}, mg/g) were estimated as follows.[16] As the adsorption reached equilibrium, the amount of CO_2 adsorbed on adsorbents (q_e, mg/g) was measured, and then the influent gas was changed to N_2 gas and controlled at a Q of 0.1 L/min. The outlet of adsorption column was connected to a vacuum pump which was operated at 65 mm-Hg. Until the CO_2 level in effluent gas streams was undetectable, the remaining weight of spent adsorbents (m_1, mg) was measured. The weight difference between m_1 and m is attributed to chemisorptions, and the q_{ec} can be estimated as

$$q_{ec} = \frac{m_1 - m}{m} \times 1000 \qquad (2)$$

The q_{ep} is thus calculated from the difference between q_e and q_{ec}.

4. Analytical Methods. CO_2 concentration was determined using a GC-TCD (model GC-2010, Shimadzu Instruments, Tokyo, Japan). A 30 m fused silica capillary column with 0.32 mm inner diameter and 5.0 μm film thickness (AB-PLOT GasPro, U.S.A.) was used for CO_2 analysis. The GC-TCD was operated at injection temperature of 50 °C, detector temperature of 100 °C, and oven temperature of 55 °C.

The morphology of adsorbents was analyzed by a high-resolution transmission electron microscope (HR-TEM, model JEM-2010, JEOL, Tokyo, Japan). The structure information of adsorbents was evaluated by a Raman spectrometer (model Nanofinder 30 R., Tokyo Instruments Inc., Tokyo, Japan). The thermal stability of adsorbents in air was determined by a thermogravimetric analyzer (TGA, model TG209 F1 Iris, NETZSCH, Bavaria, Germany) at a heating rate of 10 °C/min in the temperature range of 30–750 °C.

The physical properties of adsorbents were determined by N_2 adsorption/desorption at 77 K using Micromertics ASAP 2010 surface area and porosimetry analyzer (Norcross, GA, U.S.A.). The N_2 isotherms were measured at a relative pressure range of 0.0001–0.99 and then were employed to determine surface area of adsorbents using the Brunauer, Emmett, and Teller (BET) equation. The pore size distributions (PSDs) of adsorbents were determined from the N_2 isotherms via the Barrett, Johner, and Halenda (BJH) equation.

The chemical properties of adsorbents were determined by a Fourier transform infrared ray Spectrometer equipped with an attenuated total reflectance (FTIR/ATR) (model FTIR-SP-1 Spectrum One, Perkin-Elmer, MA, U.S.A.) and the Boehm titration.[17] The titration was conducted by adding 100 mg of adsorbents into a 100 mL flask containing 50 mL of the following 0.1 M solutions: $NaHCO_3$, Na_2CO_3, NaOH, and HCl, respectively, which were sealed and shaken at 25 °C for 48 h, and then filtered through a 0.45 μm fiber filter. The filtrate (10 mL) was pipetted and mixed with 15 mL of 0.1 M HCl or NaOH. The excess of acid and base was titrated with 0.1 M NaOH and HCl, respectively. The quantities of acidity of various types were determined from the assumption that $NaHCO_3$ reacts with carboxylic groups (−COOH), Na_2CO_3 reacts with carboxylic and lactonic groups (−COO), and NaOH reacts with carboxylic, lactonic, and phenolic groups (−OH). The quantities of total basicity were determined from the amount of HCl reacted with the adsorbents.

Results and Discussion

1. Adsorption of CO_2 with Various Modified Adsorbents. Figure 2 shows the q_e of raw and various modified adsorbents with a C_{in} of 10%. It is seen that the q_e increased
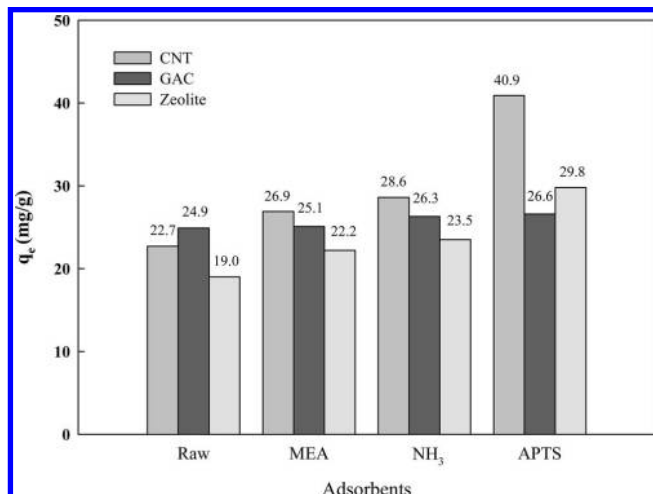
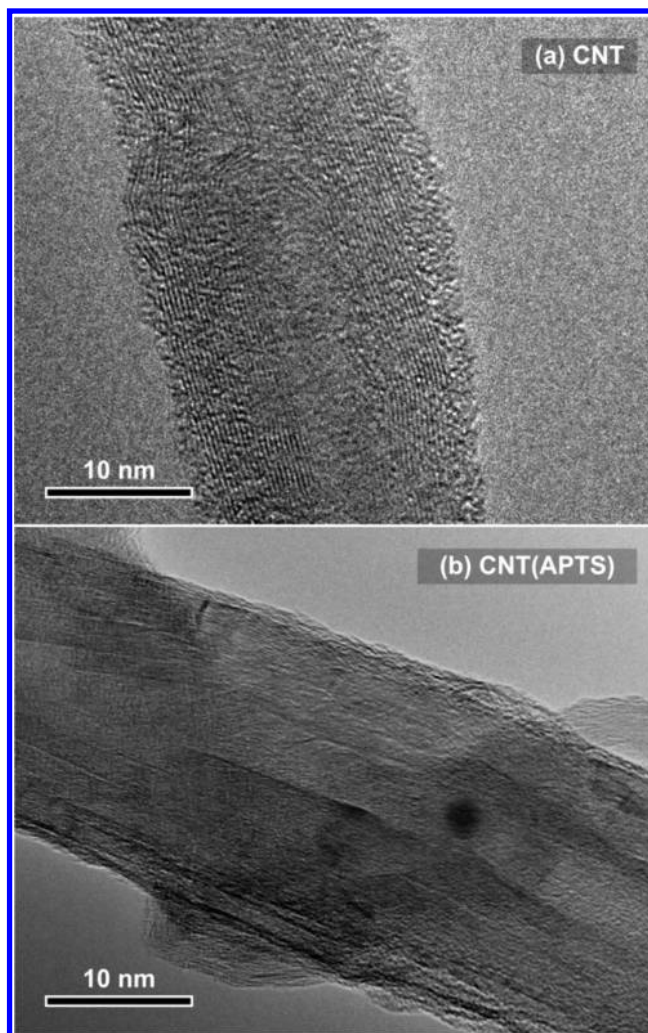**Figure 2.** Equilibrium amount of CO_2 adsorbed on various raw and modified adsorbents with a C_{in} of 10%.
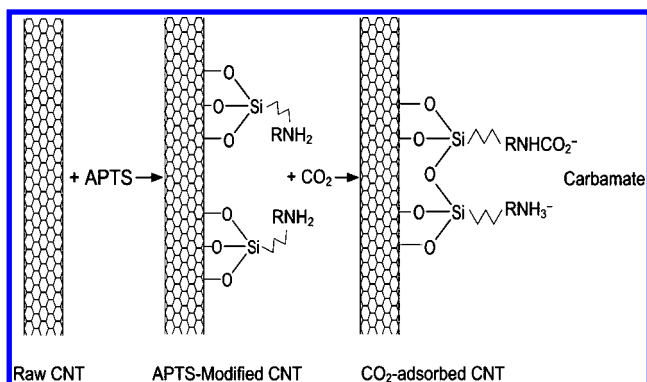
Figure 3. Diagram of the possible mechanism for chemical adsorption of CO_2 on APTS-modified CNTs in the absence of water.

Figure 4. TEM images of raw and modified CNTs.

after these adsorbents were modified by MEA, NH_3(aq), and APTS. The APTS-modified adsorbents have the greatest enhancement in q_e, followed by the NH_3-modified adsorbents and then the MEA-modified adsorbents. The raw and APTS-modified adsorbents were thus selected to study their physico-chemical properties and adsorption behaviors of CO_2 from gas streams. The possible mechanism for chemical adsorption of CO_2 on APTS-modified CNTs in the absence of water is graphically presented in Figure 3. It is seen that the capture of CO_2 by surface amine groups causes the formation of carbamate ion ($RNHCO_2^-$) and thus results in adsorbing more CO_2 gases.

2. Characterizations of Adsorbents. Figure 4 exhibits the TEM images of raw and APTS-modified CNTs. Part a shows that the isolated CNT has a multiple graphitic layers structure with an outer diameter of ∼20 nm and a hollow inner tube diameter of 4−5 nm. Part b displays that the isolated modified CNT was grafted with a thick layer of APTS. The TEM images of modified GAC and zeolites also show a thick layer of APTS grafted on their surface.

Figure 5 shows the Raman spectra of CNTs and GAC. It is obvious that there are two sharp peaks located at ∼1350 and ∼1580 cm^{-1}. The peak at 1330−1360 cm^{-1} is the D band which is related to disordered sp^2-hybidized carbon atoms of nanotubes containing vacancies, impurities, or other symmetry-breaking defects. The peak near 1580 cm^{-1} is the G band which is related to graphite E_{2g} symmetry of the interlayer mode reflecting structural integrity of sp^2-hybridized carbon atoms of the

nanotubes. Hence, the extent of carbon-containing defects of adsorbents can be evaluated by intensity ratio of the D band to G band (I_D/I_G).[18] The I_D/I_G ratios of raw and modified adsorbents are 0.496 and 0.415 for CNTs and 1.040 and 0.995 for GAC. The I_D/I_G ratio slightly decreased after the modification, indicating that the modified CNTs and GAC possess more graphitized structures and less carbon-containing defects. The raw and modified zeolites exhibit no peaks due to lack of carbon atoms.

Figure 6 reveals the TGA curves of raw and modified adsorbents. It is obvious that the TGA curves of raw CNTs and GAC show a little weight loss close to 1% below 450 and 520 °C, respectively. After that a significant weight loss begins and ends at 670 and 700 °C, in which a 4.29 and 9.22% remaining weight was found for raw CNTs and GAC, respectively. The modified CNTs and GAC have a broader temperature range for weight loss and exhibit three main weight loss regions. The first weight loss region (<550 °C) can be attributed to the evaporation of adsorbed water and the elimination of surface functional groups. The rapid weight loss region (550−620 °C for CNTs and 550−720 °C for GAC) can be assigned to the decomposition of carbon in CNTs and GAC. The third region only shows a very little weight loss close to 1%, in which 17.4 and 12.95% remaining weight was observed for CNTs and GAC, respectively. After the modification, the remaining

(16) Hsu, H.; Lu, C. *Sep. Sci. Technol.* **2007**, *42* (12), 2751–2766.
(17) Boehm, H. P. *Carbon* **1994**, *32* (5), 759–769.

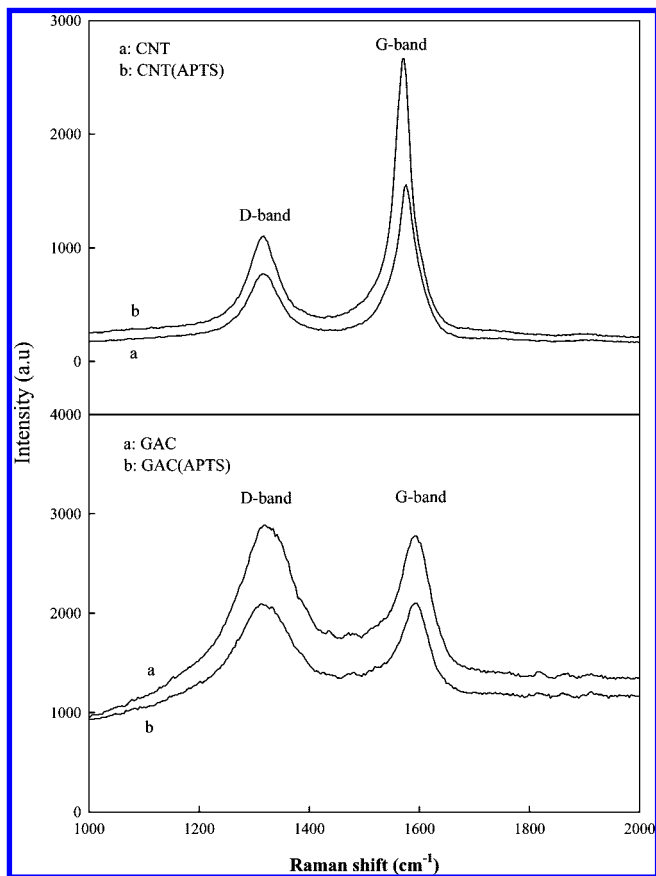(18) Tsai, C. L.; Chen, C. F. *Diamond Relat. Mater.* **2003**, *12* (9), 1615–1620.

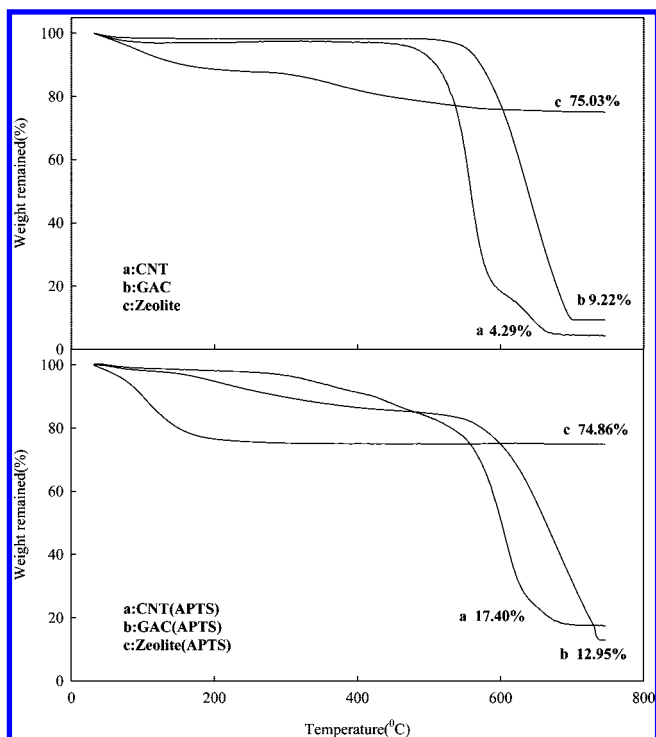**Figure 5.** Raman spectra of raw and modified CNTs and GAC.

Figure 6. TGA curves of raw and modified adsorbents.

weights of CNTs and GAC increased from 4.29 to 17.40% and from 9.22 to 12.95%, respectively, indicating that more APTS was grafted on the CNT surface. The TGA curve of raw and modified zeolites exhibits a weight loss of ~24% at 600 and 200 °C, respectively, which could be due to the evaporation of adsorbed water and the elimination of surface functional groups. After that no significant weight losses with temperature were
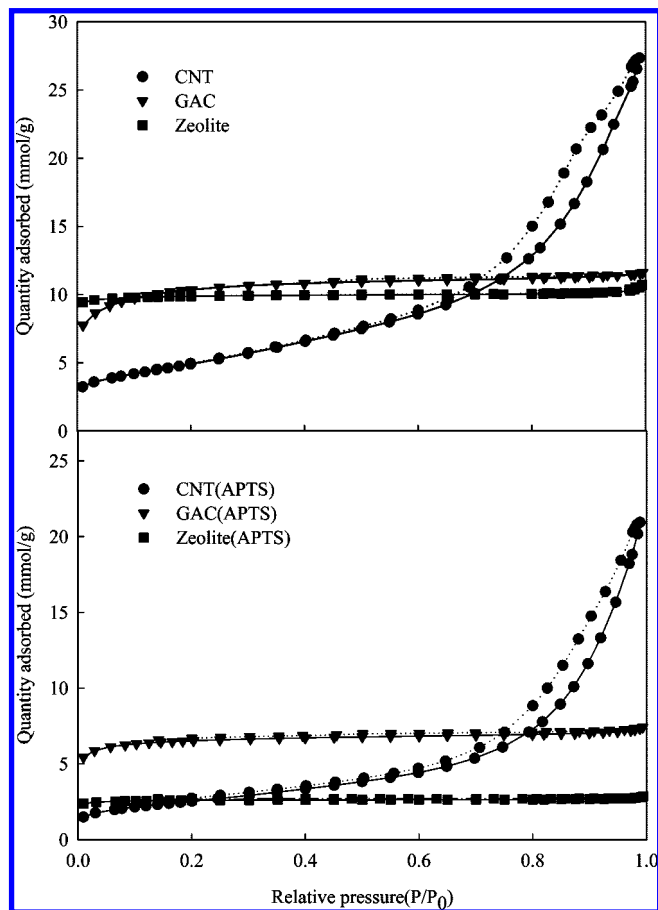

Figure 7. Adsorption (solid line) and desorption (dash line) isotherms of N_2 via raw and modified adsorbents.

observed because the gasification temperature of Si in zeolites and APTS is over the temperature range tested herein. Therefore, the C, H, and N burn off did not signal a significant weight change in TGA results on zeolites.

Figure 7 presents the adsorption/desorption isotherms of N_2 via raw and modified adsorbents. It is clear that the adsorbents have more adsorption capacity of N_2 after the modification, indicating a smaller amount of porosity within modified adsorbents due to the grafting of APTS on the adsorbent surface. The adsorption isotherms for raw and modified CNTs show a type IV shape according to IUPAC classification,[19] displaying a rise in N_2 adsorption capacity with relative pressure. This reflects that both raw and modified CNTs have a broad pore size distribution. The adsorption/desorption isotherms of N_2 via raw and modified GAC and zeolites are approximately type I, which is classified as the Langmuir type and is characterized by the formation of a complete monolayer. After a sharp increase up to relative pressure of 0.1, the adsorption isotherms show a very small increment with relative pressure, indicating that the GAC and zeolites have small pores and their pore size distributions are very narrow. The adsorption/desorption isotherms of GAC and zeolites nearly coincide with each other, implying the absence of adsorption hysteresis.
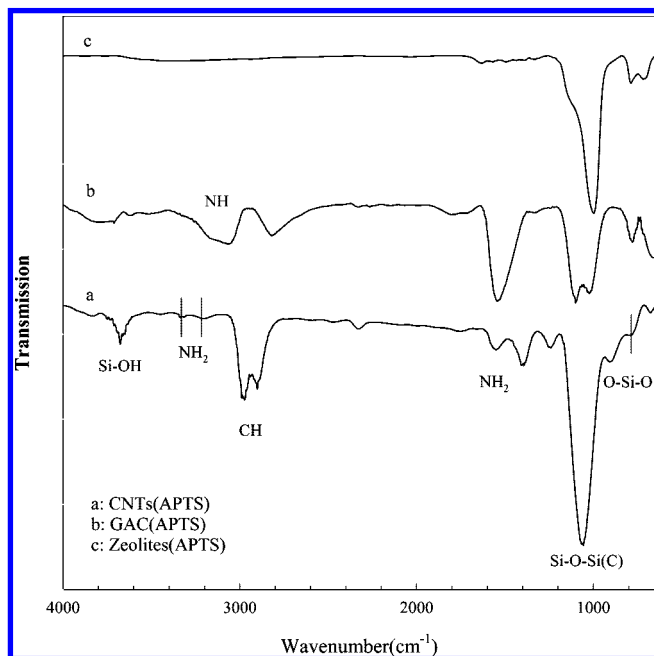
The physical properties of raw and modified adsorbents are given in Table 1. It is seen that the pore structure of adsorbents partially changed after the modification, which results in the decrease in the surface area and pore volume but a rise in average pore diameter. This could be explained by the grafting of APTS on the small pores of adsorbents. Most pore volumes

(19) Gregg, S. J.; Sing, K. S. W. *Adsorption, Surface Area and Porosity*; Academic Press: New York, 1982.

Table 1. Physical Properties of Raw and Modified Adsorbents[a]

adsorbents	SA	APD	PV	% of total PV in stated pore size (nm) range		
				1.7−5	5−20	>20
CNT	394	8.9	0.91	54.2	43.9	1.9
CNT(APTS)	198	12.2	0.63	31.7	63.5	4.8
GAC	954	2.0	0.48	96.6	3.3	0.1
GAC(APTS)	508	2.02	0.25	95.6	4.1	0.3
Zeolite	788	1.89	0.35	92.5	6.3	1.2
Zeolite(APTS)	203	1.95	0.09	97.7	1.1	1.2

[a] Note: SA, surface area (m^2/g); APD, average pore diameter (nm); PV, pore volume (cm^3/g).

Table 2. Results of Boehm Titration[a]

adsorbents	carboxylic groups	lactonic groups	phenolic groups	total acidity	total basicity
CNT	1.137	ND	0.675	1.812	1.20
CNT(APTS)	1.227	0.377	0.200	1.804	2.290
GAC	0.791	0.480	0.549	1.820	1.10
GAC(APTS)	0.816	0.679	0.253	1.748	1.45
Zeolite	0.884	0.263	0.706	1.853	0.96
Zeolite(APTS)	1.069	0.331	0.418	1.818	1.82

[a] Unit: mmol/g.

Figure 8. IR spectra of modified adsorbents.
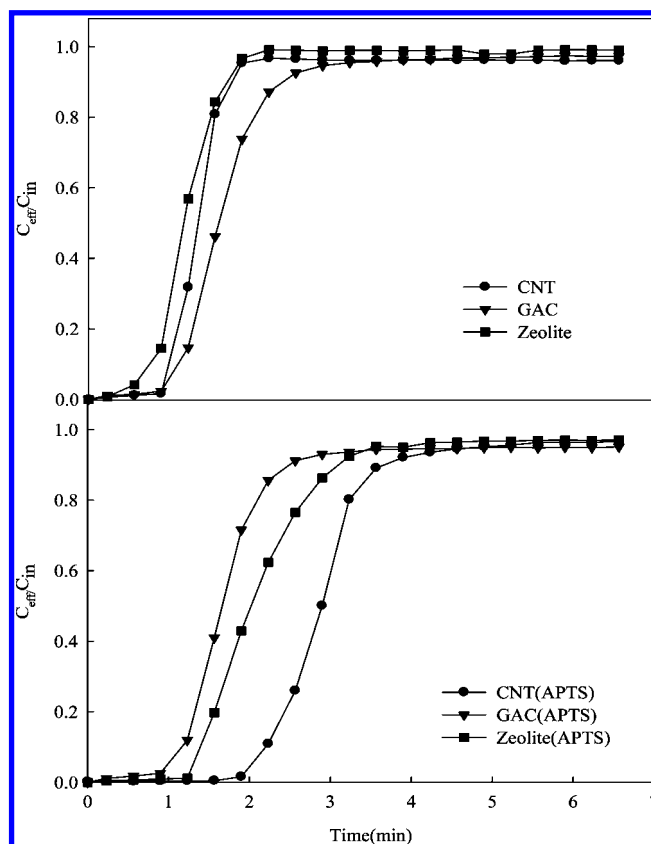
Figure 9. Breakthrough curves of CO_2 adsorption via raw and modified adsorbents with a C_{in} of 50%.

of modified CNTs are in the 5−20 nm size range while most pore volumes of raw and modified GAC and zeolites are in the size range of 1.7−5 nm. It must be noted that the low detection limit for pore size of the employed BET analyzer is around 1.7 nm. Therefore, a quantification of the inner diameter distribution of adsorbents less than 1.7 nm is not possible in this study.

Figure 8 displays the IR spectra of modified adsorbents. It is observed that the IR spectra of modified CNTs exhibit several significant bands at 3674, 3200−3305, 2900−2971, 1391−1560, 1000−1200, and 800 cm^{-1} which are associated with bridge Si−OH acidic groups,[20] asymmetric and symmetric NH_2 stretching −OH, CH stretching from $CH_2CH_2CH_2$−NH_2 groups,[21] NH_2 deformation of hydrogen bonded amine group,[22] and Si−O−Si(C)[23] and O−Si−O vibrations,[24] respectively. The abundance of these surface amine functional groups can provide numerous chemical adsorption sites for CO_2 capture. The modified GAC has the remarkable bands at 3101, 1530, and 1020−1081 cm^{-1} while the modified zeolites have the profound band at 1054 cm^{-1}.

The results of Boehm titration are given in Table 2. It is seen that the amounts of carboxylic and lactonic groups increased but the amounts of phenolic groups decreased after the modification. The decrease in phenolic groups could be explained by the reaction between APTS and phenolic groups on silica during the modification. Similar findings have been reported in the literature.[22] The total basicity of adsorbents, which can be related to the chemical adsorption site for CO_2 capture, increased after the modification due to the grafting of amine groups on the adsorbent surface. The total basicity is in the following order: CNTs > GAC > zeolites for raw adsorbents and CNTs > zeolites > GAC for modified adsorbents.

3. Adsorption Behaviors. Figure 9 shows the breakthrough curves of CO_2 adsorption via raw and modified adsorbents with a C_{in} of 50%. It is evident that initially the CO_2 can be efficiently adsorbed on adsorbents with capture efficiencies >96%. The breakthrough times, the time at which effluent CO_2 concentration reaches 5% allowable breakthrough concentration, are in the following order: GAC > CNTs > zeolites for raw adsorbents and CNTs > zeolites > GAC for modified adsorbents. The breakthrough time becomes longer after the modification, and the modified CNTs were found to be the best of these adsorbents to achieve high CO_2 capture.

(20) Ha, V. T. T.; Tiep, L. V.; Meriaudeau, P.; Naccache, C. *J. Mol. Catal. A* **2002**, *181* (1−2), 283−290.

(21) Chang, A. C. C.; Chuang, S. S. C.; Gray, M.; Soong, Y. *Energy Fuels* **2003**, *17* (2), 468−473.

(22) Huang, H. Y.; Yang, R. T.; Chinn, D.; Munson, C. L. *Ind. Eng. Chem. Res.* **2003**, *42* (12), 2427−2433.

(23) Jing, S.; Lee, H.; Choi, C. *J. Korean Chem. Soc.* **2002**, *41* (5), 769−773.

(24) Zhang, C.; Liu, Q.; Xu, Z. *J. Non-Cryst. Solids* **2005**, *351* (16−17), 1377−1382.
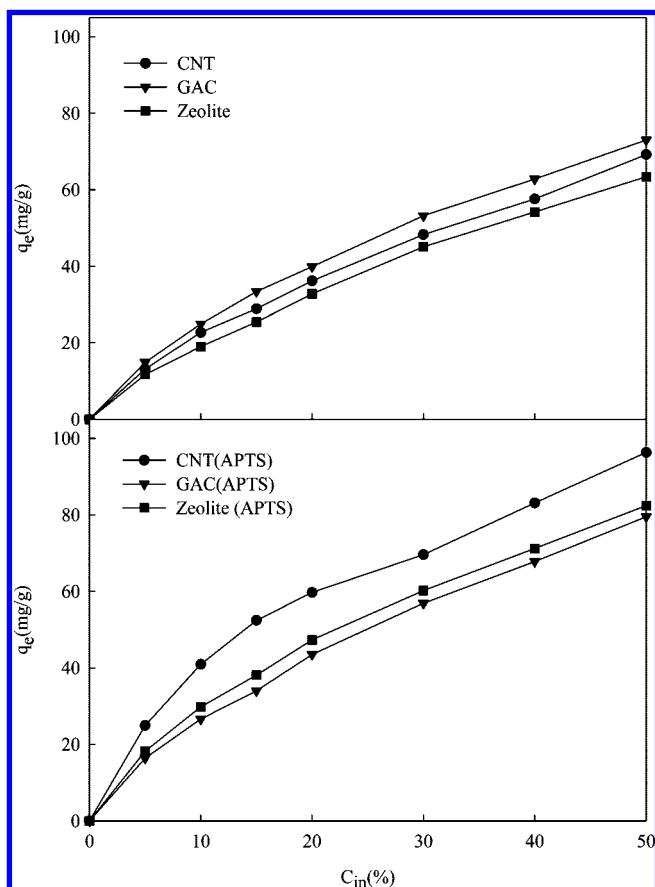
Figure 10. Adsorption isotherms of CO_2 via raw and modified adsorbents.
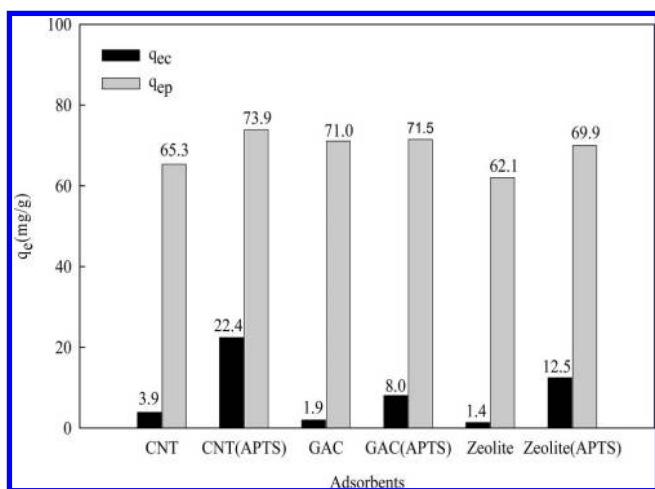
Figure 11. Physisorption and chemisorption capacities of CO_2 via raw and modified adsorbents with a C_{in} of 50%.

Figure 10 shows the adsorption isotherms of raw and modified adsorbents with a C_{in} range of 5–50%. It is seen that the q_e increased with C_{in} and was enhanced after the modification. With a C_{in} of 50%, the q_e of CNTs, GAC, and zeolites respectively are 69.2, 72.9, and 63.5 mg/g for raw adsorbents and 96.3, 79.5, and 82.4 mg/g for modified adsorbents. The CNTs show the greatest enhancement in q_e (27.1 mg/g), followed by the zeolites (18.9 mg/g) and then the GAC (6.6 mg/g).

Figure 11 shows the q_{ec} and q_{ep} of raw and modified adsorbents with a C_{in} of 50%. It is evident that both q_{ec} and q_{ep}

Table 3. Comparisons of q_e via Various Raw and Modified Adsorbents

adsorbents	grafting agents	q_e (mg/g)	conditions	references
CNTs	APTS[a]	40.9	$C_{in} = 10\%, T = 25\ °C$	this work
	APTS	96.3	$C_{in} = 50\%, T = 25\ °C$	
activated carbon		53	$C_{in} = 99\%, T = 36\ °C$	8
	NH₃	77		
SBA-15		2.2	$C_{in} = 15\%, T = 60\ °C$	12
	APTS	6.6		
SWCNT		87	$C_{in} = 99\%, T = 35\ °C$	13
SBA-15	APTS	9.9	$C_{in} = 4\%, T = 25\ °C$	21
silica xerogel	APTS	25	$C_{in} = 5\%, T = 25\ °C$	22
amorphous silica gel	TA[b]	46	$C_{in} = 90\%, T = 20\ °C$	25
MCM41	PEI[c]	19	$C_{in} = 99\%, T = 75\ °C$	26
SBA-15	EDA[d]	20	$C_{in} = 15\%, T = 25\ °C$	27

[a] APTS = 3-aminopropyl-triethoxysilane. [b] TA = N-[3-(trimethoxysilyl)-propyl]diethylenetriamine. [c] PEI = polyethylenimine. [d] EDA = N-[3-(trimethoxysilyl)propyl]ethylenediamine.

increased after the modification. The CNTs exhibit the greatest enhancement in q_{ec} and q_{ep}, followed by the zeolites and then the GAC. The q_{ep} values are much higher than the q_{ec} values, indicating that the mechanism of CO_2 adsorption on these adsorbents appears mainly attributable to physical force, which makes the regeneration process of CO_2 at a relatively low temperature become feasible. The increase in q_{ep} could be attributed to the increase in affinity between CO_2 molecules and adsorbent surface while the increase in q_{ec} could be explained by the increase in total basicity and surface amine groups as shown in Table 2 and Figure 8, respectively.

The effect of relative humidity (RH) on the adsorption of CO_2 via modified CNTs was evaluated with a C_{in} of 50%. Moisture was introduced into the gas stream by dispersing the diluting gas through a water bath before being mixed with pure CO_2 gas. The results indicated that the q_e slightly increased with a rise in RH, which could be explained by the fact that with the adsorption of water on the surface of modified CNTs may cause the dissolution of CO_2 into water. Furthermore, the carbamate ion formed in reaction of CO_2 and surface amine groups may further react with CO_2 and H_2O to form bicarbonate ion (HCO_3^-), or the amine groups themselves can also directly react with CO_2 and H_2O to form HCO_3^-. Similar findings have been reported in the literature for adsorption of CO_2 on polyethylenimine-modified MCM41.[15]

4. Comparison with Literature Results. The comparisons of q_e via various raw and modified adsorbents are given in Table 3. Different adsorbents such as silica xerogel, SWCNT, SBA-15, MCM41, and activated carbon have been reported and modified by various kinds of grafting agents such as APTS, PEI, NH₃, EDA, and TA. It is apparent that the q_e of these adsorbents can be usually be enhanced after the modification. Under analogous conditions, the APTS-modified CNTs possess good performance of CO_2 adsorption as compared to those reported in the literature, reflecting that the APTS-modified CNTs are promising adsorbents for CO_2 capture from gas streams. And as the costs of commercially available CNTs are continuously decreasing, it is possible to utilize these novel materials in the near future.

Conclusions

The raw and APTS-modified CNTs, GAC, and zeolites were selected as adsorbents to study their physicochemical properties

(25) Knowles, G. P.; Delaney, S. W.; Chaffee, A. L. *Ind. Eng. Chem. Res.* **2006**, *45* (8), 2626–2633.

(26) Xu, X.; Song, C.; Andresen, J. M.; Miller, B. G.; Scaroni, A. W. *Microporous Mesoporous Mater.* **2003**, *62* (1–2), 29–45.

and adsorption behaviors of CO_2 from gas streams. The surface nature of these adsorbents was changed after the modification including the increase in affinity between CO_2 molecules and adsorbent surface and the increase in total basicity and amine groups, which makes these adsorbents that adsorb more CO_2 gases. After the modification, the CNTs show the greatest enhancement in adsorption capacity of CO_2, followed by the zeolites and then the GAC. Under analogous conditions, the APTS-modified CNTs have good performance of CO_2 adsorption as compared to many types of carbon and silica adsorbents reported in the literature, reflecting that the APTS-modified CNTs are promising adsorbents for CO_2 capture from gas streams. The adsorption mechanism of CO_2 appears principally attributable to physical force, which makes the regeneration process of CO_2 at a relatively low temperature become feasible and thus reduces a significant amount of energy requirement. Further work is currently underway to investigate the reversibility of CO_2 adsorption by these adsorbents.

(27) Zheng, F.; Tran, D. N.; Busche, B. J.; Fryxell, G. E.; Addleman, R. S.; Zemanian, T. S.; Aardahl, C. L. *Ind. Eng. Chem. Res.* **2005**, *44* (9), 3099–3105.